Supplement to "Atmospheric and Watershed Modelling of Trifluoroacetic Acid from Oxidation of HFO-1234ze(E) Released by Prospective Pressurized Metered-Dose Inhaler in Three Major River Basins"

By

Shivendra G. Tewari[1,*], Krish Vijayaraghavan[2], Kun Zhao[2], Liji M. David[2], Katie Tuite[2], Felix Kristanovich[2], Yuan Zhuang[2], Benjamin Yang[2], Cecilia Hurtado[2], Dimitrios K. Papanastasiou[3], Paul Giffen[4], Holly Kimko[1], Megan Gibbs[1], Stefan Platz[5]

[1]Clinical Pharmacology & Quantitative Pharmacology, R&D BioPharmaceuticals, AstraZeneca, Gaithersburg, USA

[2]Ramboll, Novato, USA

[3]Honeywell, Buffalo, USA

[4]Clinical Pharmacology & Safety Sciences, R&D BioPharmaceuticals, AstraZeneca, Cambridge, UK

[5]Clinical Pharmacology & Safety Sciences, R&D BioPharmaceuticals, AstraZeneca, Baar, Switzerland

Running Head: HFO-1234ze(E) emissions form negligible surface-water TFA

*Address correspondence to: shivendra.tewari@astrazeneca.com

Table S1. Degradation mechanism for HFO-1234ze(E).

S.N.	Master-Chemical Mechanism	In Geos-Chem?	Implementation in Geos-Chem	Rate constant (cm^3 $molecule^{-1}$ s^1)	Note
First-generation chemistry					
1.	$CF_3CHCHF + OH (+O_2) \rightarrow RPO_2$	Y[1]	$CF_3CHCHF + OH \rightarrow FRO2$	6.17×10^{-13} exp(37/T)	(a)
2.	$CF_3CHCHF + OH (+O_2) \rightarrow RSO_2$	Y[1]			(a)
3.	$RPO_2 + NO \rightarrow RPO + NO_2$	Y[1]	$FRO_2 + NO \rightarrow CF_3CHO + HCOF + HO_2 + NO_2$	$1.6*2.7\times10^{-12}$ exp(360/T)	(b)
4.	$RPO_2 + NO_3 \rightarrow RPO + NO_2 + O_2$	N			(c)
5.	$RPO_2 + HO_2 \rightarrow RPOOH + O_2$	N			(c)
6.	$RPO_2 + HO_2 \rightarrow RPCO + H_2O + O_2$	Y[1]	$FRO2 + HO_2 \rightarrow FRCO$	$0.7*3.88\times10^{-13}$ exp(800/T)	(d)
7.	$RPO_2 (+ RO_2) \rightarrow RPO (+ RO_2 + O_2)$	N			(c)
8.	$RSO_2 + NO \rightarrow RSO + NO_2$	Y[1]			(b)
9.	$RSO_2 + NO_3 \rightarrow RSO + NO_2 + O_2$	N			(e)
10.	$RSO_2 + HO_2 \rightarrow RSOOH + O_2$	N			(e)
11.	$RSO_2 + HO_2 \rightarrow RSCO + H_2O + O_2$	Y[1]			(d)
12.	$RSO_2 (+ RO_2) \rightarrow RSO (+ RO_2 + O_2)$	N			(e)
13.	$RPO \rightarrow CF_3CHO + HCOF + HO_2$	Y[1]			(b)
14.	$RSO \rightarrow CF_3CHO + HCOF + HO_2$	Y[1]			(b)
Degradation of other first-generation products					
15.	$RPOOH + OH \rightarrow RPO_2 + H_2O$	N			(f)
16.	$RPOOH + OH \rightarrow RPCO + OH$	N			(f)
17.	$RPOOH \rightarrow RPO + OH$	N			(f)
18.	$RPCO + OH (+O_2) \rightarrow CF_3COCOF + HO_2$	Y[1]	$FRCO + OH \rightarrow CF_3C(O)C(O)F + HO_2$	4.87×10^{-13} exp(-73/T)	(g)
19.	$RPCO + OH (+O_2) \rightarrow CF_3CHO + FCO_3$	N			(h)
20.	$RSOOH + OH \rightarrow RSO_2 + H_2O$	N			(i)

S.N.	Master-Chemical Mechanism	In Geos-Chem?	Implementation in Geos-Chem	Rate constant (cm^3 $molecule^{-1}$ s^1)	Note
21.	RSOOH + OH --> RSCO + OH	N			(i)
22.	RSOOH --> RSO + OH	N			(i)
23.	RSCO + OH (+O_2) --> CF_3COCOF + HO_2	Y^1	FRCO + OH --> CF_3CHO + FCO_3	1.28×10^{-12} exp(-660/T)	(g)
24.	RSCO + OH (+O_2) --> CF_3CO_3 + HCOF	N			(h)
25.	CF_3COCOF (+2O_2) --> CF_3CO_3 + FCO_3	Y	$CF_3C(O)C(O)F$ + hν --> $CF_3C(O)O_2$	λ-dependent σ for $CH_3C(O)CHO$	(j)
Degradation of CF_3CHO (TFAA) with OH					
26.	CF_3CHO + OH (+O_2) --> CF_3CO_3 + H_2O	Y	CF_3CHO + OH (+O_2) --> $CF_3C(O)O_2$	1.8×10^{-12} exp(-343/T)	(k) Major TFA formation pathway.
27.	CF_3CHO (+2O_2) --> CF_3O_2 + CO + HO_2	Y	CF_3CHO + hν --> CO_2 + HF	λ-dependent σ	(l) Major TFAA loss process.
28.	CF_3CO_3 + NO --> CF_3O_2 + NO_2	Y	$CF_3C(O)O_2$ + NO --> $CF_3C(O)O$ + NO_2	4.0×10^{-12} exp(560/T)	(m)
29.	CF_3CO_3 + NO_3 --> CF_3O_2 + NO_2 + O_2	N			(n)
30.	CF_3CO_3 + HO_2 --> CF_3CO_3H + O_2	Y	$CF_3C(O)O_2$ + HO_2 --> $CF_3C(O)OOH$	0.08*1.7×10^{-12} exp(730/T)	(m)
31.	CF_3CO_3 + HO_2 --> TFA + O_3	Y	$CF_3C(O)O_2$ + HO_2 --> $CF_3C(O)OH$ + O_3	0.38*1.7×10^{-12} exp(730/T)	Major TFA formation pathway.
32.	CF_3CO_3 + HO_2 --> CF_3O_2 + OH + O_2	Y	$CF_3C(O)O_2$ + HO_2 --> $CF_3C(O)O$ + OH	0.54*1.7×10^{-12} exp(730/T)	(m)
33.	CF_3CO_3H --> CF_3O_2 + OH	N			(o)
34.	CF_3CO_3 + NO_2 (+ M) --> TFPAN (+ M)	Y	$CF_3C(O)O_2$ + NO_2 (+M) --> $CF_3C(O)OONO_2$ (+M)	$k_0 = 2.13\text{x}10^{-27}\left(\frac{T}{300}\right)^{-6.87}$ [M] $k_1 = 6.6\text{x}10^{-12}\left(\frac{T}{300}\right)^{-1.105}$ $k_r = k_0/k_1$	(m)

S.N.	Master-Chemical Mechanism	In Geos-Chem?	Implementation in Geos-Chem	Rate constant (cm^3 $molecule^{-1}$ s^1)	Note
				$f = 10^{1+\frac{\frac{\log(0.2)}{\log(k_r)}^2}{0.75-1.27*\log(0.2)}}$ $k = \frac{k_0 * k_1 * f}{k_0+k_1}$	
35.	TFPAN (+ M) --> CF_3CO_3 + NO_2 (+ M)	Y	$CF_3C(O)OONO_2$ (+M) --> $CF_3C(O)O_2$ + NO_2 (+M)	$k_0 = 5.0x10^{-2} \exp(\frac{-12350}{T})$ [M] $k_1 = 1.1x10^{17} \exp(\frac{-14440}{T})$ $k_r = k_0/k_1$ $f = 10^{1+\frac{\frac{\log(0.2)}{\log(k_r)}^2}{0.75-1.27*\log(0.2)}}$ $k = \frac{k_0 * k_1 * f}{k_0+k_1}$	(p)
36.	TFPAN --> CF_3O_2 + NO_3	Y^1	$CF_3C(O)OONO_2$ + hν --> 0.5*$CF_3C(O)O_2$ + 0.5*NO_2 + 0.5*$CF_3C(O)O$ + 0.5*NO_3	λ-dependent σ for $CH_3C(O)OONO_2$, red-shifted by 5 nm	(q)
37.	TFPAN --> CF_3CO_3 + NO_2	Y^1			(q)
38.	CF_3CO_3 (+ RO_2) --> CF_3O_2 (+ RO + O_2)	Y	$CF_3C(O)O_2$ + CH_3O_2 --> $CF_3C(O)O$	$0.9*2.0\times10^{-12}$ exp(508/T)	(r)
39.	CF_3CO_3 (+ RO_2) --> TFA (+ R_HO + O_2)	Y	$CF_3C(O)O_2$ + CH_3O_2 --> $CF_3C(O)OH$ + HO_2	$0.1*2.0\times10^{-12}$ exp(508/T)	(r)
Other chemistry					
40.	CF_3O_2 + NO --> CF_3O + NO_2	N			(s)
41.	CF_3O_2 + NO_3 --> CF_3O + NO_2 + O_2	N			
42.	CF_3O_2 + HO_2 --> CF_3OOH + O_2	N			
43.	CF_3O_2 + HO_2 --> COF_2 + HOF + O_2	N			
44.	CF_3O_2 + (RO_2) --> CF_3O (+RO + O_2)	N			
45.	CF_3O + NO --> COF2 + FNO	N			
46.	CF_3O + O_3 --> CF_3O_2 + O_2	N			
47.	CF_3O --> CF_3OH	N			
48.	FCO_3 + NO --> FCO_2 + NO_2	N			
49.	FCO_2 + NO --> FNO + CO_2	N			
Degradation of CF_3CHO (TFAA) with HO_2					

S.N.	Master-Chemical Mechanism	In Geos-Chem?	Implementation in Geos-Chem	Rate constant (cm^3 $molecule^{-1}$ s^1)	Note
50.	$CF_3CHO + HO_2$ --> HRO_2	Y	$CF_3CHO + HO_2$ --> $CF_3CH(OH)O_2$	8.0×10^{-16} exp(1707/T)	(t)
51.	HRO_2 --> $CF_3CHO + HO_2$	Y	$CF_3CH(OH)O_2$ --> $CF_3CHO + HO_2$	1.75×10^{12} exp(-6179/T)	(u)
52.	$HRO_2 + NO$ --> $HRO + NO_2$	Y[1]	$CF_3CH(OH)O_2 + NO$ --> $0.5*HCOOH + 0.5*CF_3C(O)O + 0.5*CF_3C(O)OH + 0.5*HO_2 + NO_2$	$1.6*2.7\times10^{-12}$ exp(360/T)	(t), (v)
53.	$HRO_2 + NO_3$ --> $HRO + NO_2 + O_2$	N			(w)
54.	$HRO_2 + HO_2$ --> $HROOH + O_2$	Y[1]	$CF_3CH(OH)O_2 + HO_2$ --> $0.5*CF_3CH(OH)OOH + 0.5*CF_3C(O)OH + 0.2*OH + 0.2*HO_2$	5.25×10^{-12} exp(800/T)	(x)
55.	$HRO_2 + HO_2$ --> $TFA + H_2O + O_2$	Y[1]			(x)
56.	$HRO_2 + HO_2$ --> $TFA + OH + HO_2$	Y[1]			(x)
57.	HRO_2 (+ RO_2) --> HRO (+ $RO + O_2$)	N			(w)
58.	HRO_2 (+ RO_2) --> TFA (+ $ROH + O_2$)	N			(w)
59.	HRO_2 (+ RO_2) --> $HROH$ (+ $R_{-H}O + O_2$)	N			(w)
60.	$HROOH + OH$ --> $TFA + OH + H_2O$	Y	$CF_3CH(OH)OOH + OH$ --> $CF_3C(O)OH + OH$	7.83×10^{-13} exp(167/T)	(y)
61.	$HROOH + OH$ --> $HRO_2 + H_2O$	Y	$CF_3CH(OH)OOH + OH$ --> $CF_3CH(OH)O_2$	3.68×10^{-13} exp(635/T)	(y)
62.	$HROOH$ --> $HRO + OH$	Y[1]	$CF_3CH(OH)OOH + h\nu$ --> $0.5*CF_3C(O)O + 0.5*HCOOH + 0.5*CF_3C(O)OH + 0.5*HO_2 + OH$	λ-dependent σ for CH_3OOH	(y), (z)
63.	$HROH + OH$ --> $HRO + H_2O$	N			(aa)
64.	$HROH + OH$ (+ O_2) --> $TFA + HO_2$	N			(aa)
65.	HRO (+ O_2) --> CF_3O_2 + $HCOOH$	Y[1]			(v), (z)
66.	HRO (+ O_2) --> $TFA + HO_2$	Y[1]			(v), (z)
Degradation of TFA (gas phase)					
67.	$TFA + OH$ (+ O_2) --> $CF_3O_2 + CO_2$	Y	$CF_3C(O)OH + OH$ --> CF3C(O)O	9.35×10^{-14} (Hurley et al. 2008)	Major TFA (gas phase) loss

S.N.	Master-Chemical Mechanism	In Geos-Chem?	Implementation in Geos-Chem	Rate constant (cm^3 $molecule^{-1}$ s^1)	Note
					pathway.
Wet and dry deposition of TFA					
	N/A		Dry and wet deposition will be included.		

[1] Combined with other reactions for GEOS-Chem mechanism; see the Notes/Justification column for details.

(a) A major TFA formation pathway. Reactions 1 and 2 are combined into a single reaction in GEOS-Chem. FRO2 collectively represents the peroxy radicals formed from CF_3CHCHF oxidation.

(b) Reactions 3, 8, 13, and 14 are combined into a single reaction in GEOS-Chem. Rate constant based on IUPAC recommendation for similar species.

(c) Only relevant in absence of NO; Rate constant ~10x smaller than RPO2+NO.

(d) Reactions 6 and 11 are combined into a single reaction in GEOS-Chem. Hydroxy-carbonyls (FRCO) are the major product in FRO2+HO2 reaction. Rate constant based on IUPAC recommendation for similar species.

(e) Only relevant in absence of NO; Rate constant ~10x smaller than RSO2+NO.

(f) Chemical pathway not relevant with removal of RPO2+HO2→RPOOH.

(g) Reactions 18 and 23 are combined into a single reaction in GEOS-Chem.

(h) Minor oxidation pathway; Oxidation lifetime is ~4 weeks so likely reactant will be removed by wet deposition prior to reaction with OH.

(i) Chemical pathway not relevant with removal of RSO2+HO2→RSOOH.

(j) FCO_3 product does not impact TFA formation so is excluded to simplify mechanism.

(k) Rate constant based on IUPAC recommendation for similar species. Reaction involves two steps:

CF3CHO + OH → CF3CO + H2O

CF3CO + O2 + M → CF3(O)O2 + M

Low TFA yield following further reaction of CF_3CO; influenced by NO_x concentration.

(l) Photolysis occurs via several steps but does not lead to TFA formation so only the first step is included.

(m) Competes with TFA formation pathway ($CF_3(O)O_2 + HO_2$).

(n) Only relevant in absence of NO; Rate constant ~10x smaller than CF_3CO_3+NO.

(o) CF_3CO_3H formation in CF_3CO_3+HO_2 reaction is minor.

(p) TFPAN acts as reservoir species for CF_3CO_3, with a lifetime of <1 day in the tropospheric boundary to several months at about 5 km.

(q) Reactions 36 and 37 are combined into a single reaction in GEOS-Chem.

(r) RO_2 approximated with CH_3O_2 in GEOS-Chem.

(s) These reactions do not lead to TFA formation.

(t) Can lead to TFA formation at low temperatures in the upper troposphere.

(u) HRO_2 undergoes rapid thermal decomposition at most atmospheric temperatures but slows in upper troposphere.

(v) Reactions 52, 65, and 66 are combined into a single reaction in GEOS-Chem. Rate constant based on IUPAC recommendation for similar species.

(w) Not with competitive as HRO_2+NO and HRO_2+HO_2 reactions.

(x) Reactions 54, 55, and 56 are combined into a single reaction in GEOS-Chem. Rate constant based on IUPAC recommendation for similar species.

(y) Impacts TFA formation from HRO_2+HO_2 reaction.

(z) Reactions 62, 65, and 66 are combined into a single reaction in GEOS-Chem.

(aa) Not relevant with removal of HRO2+RO2 reaction.

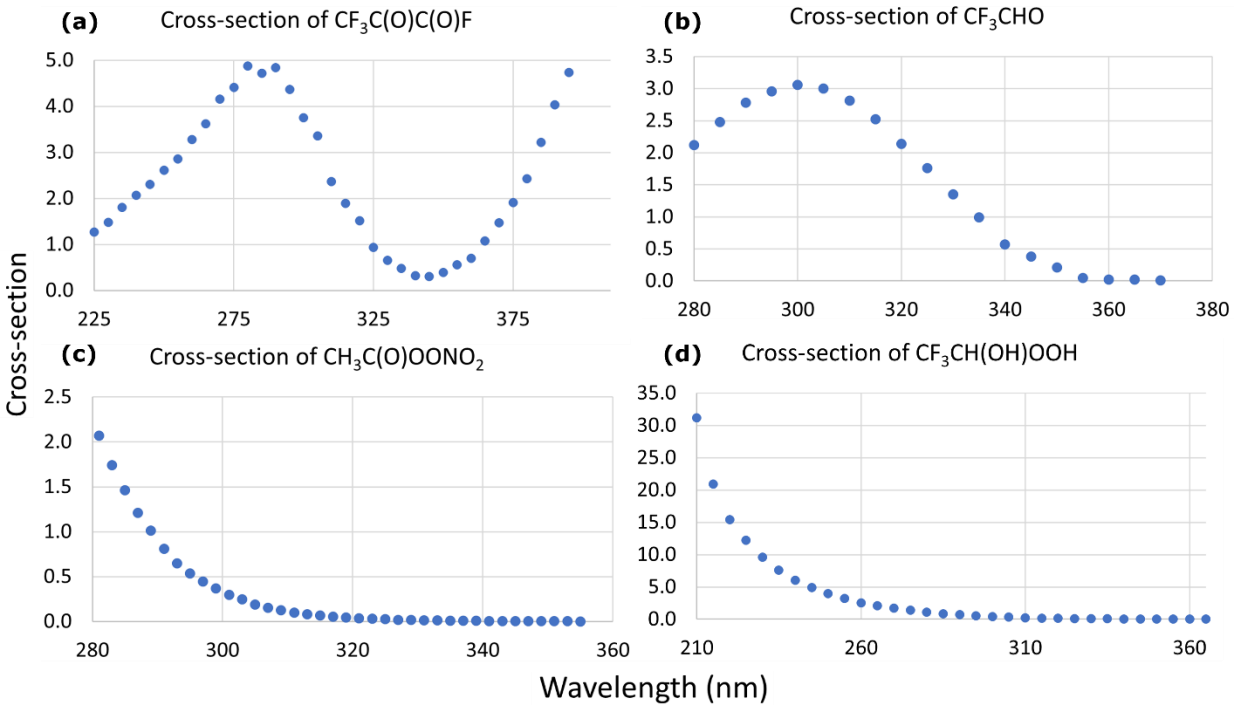

Fig. S1. Wavelength varying cross-sections (10^{-20} cm^2 $molecule^{-1}$) of (a) $CF_3C(O)C(O)F$, (b) CF_3CHO, (c) $CF_3C(O)OONO_2$, and (d) $CF_3CH(OH)OOH$.

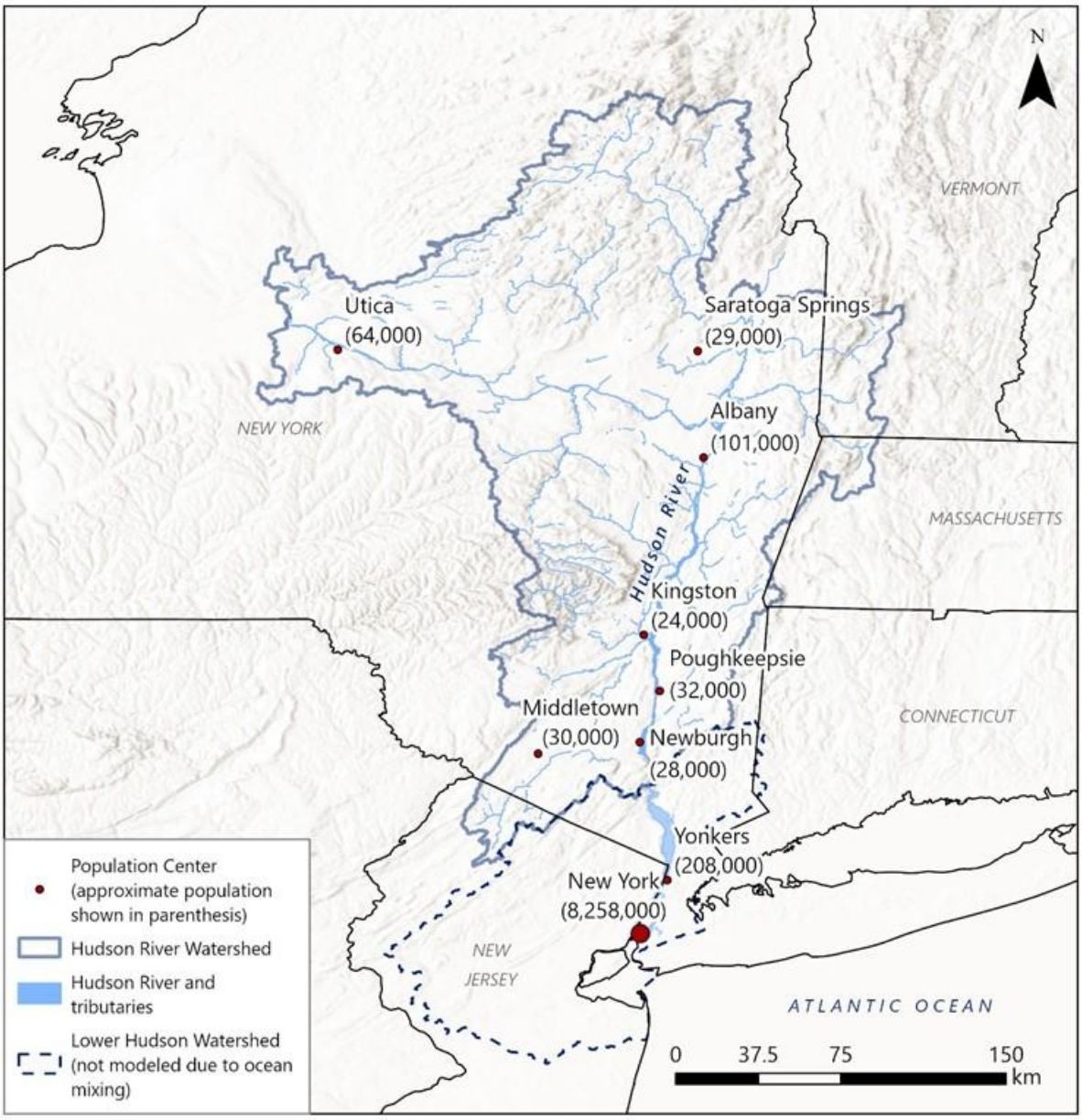

Fig. S2: Hudson River watershed with population centres. The U.S. populations are based on the 2023 population estimates from the U.S. Census Bureau. State shapefiles are from https://www.census.gov/geographies/mapping-files/time-series/geo/carto-boundary-file.html. Watershed boundaries and river/tributaries shapefile: National Hydrography Dataset, https://apps.nationalmap.gov/downloader/. Population data is from US Census Bureau, https://www.census.gov/quickfacts/.

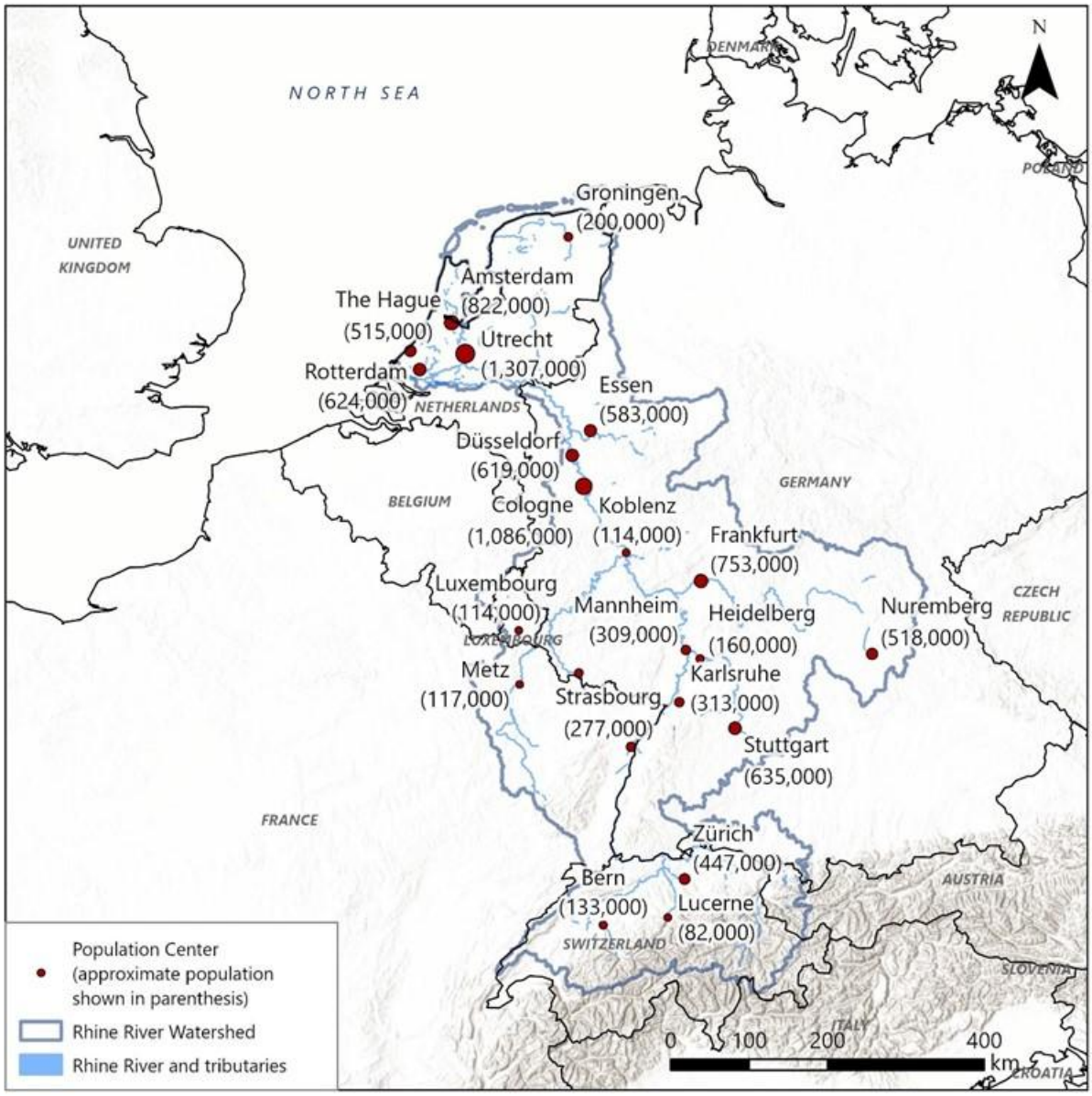

Fig. S3: Rhine River watershed with population centres. The European Union population estimates are based on Eurostat estimates provided for 2015, 2017, or 2019, depending on the country. Countries shapefile: Urbano, Ferdinando (2018): Global administrative boundaries. European Commission, Joint Research Centre (JRC) [Dataset] PID: http://data.europa.eu/89h/jrc-10112-10004. Watershed boundaries and river/tributaries shapefile: EU-Hydro River Network Database: https://land.copernicus.eu/imagery-in-situ/eu-hydro/eu-hydro-river-network-database?tab=download. Population data: ec.europa.eu/Eurostat

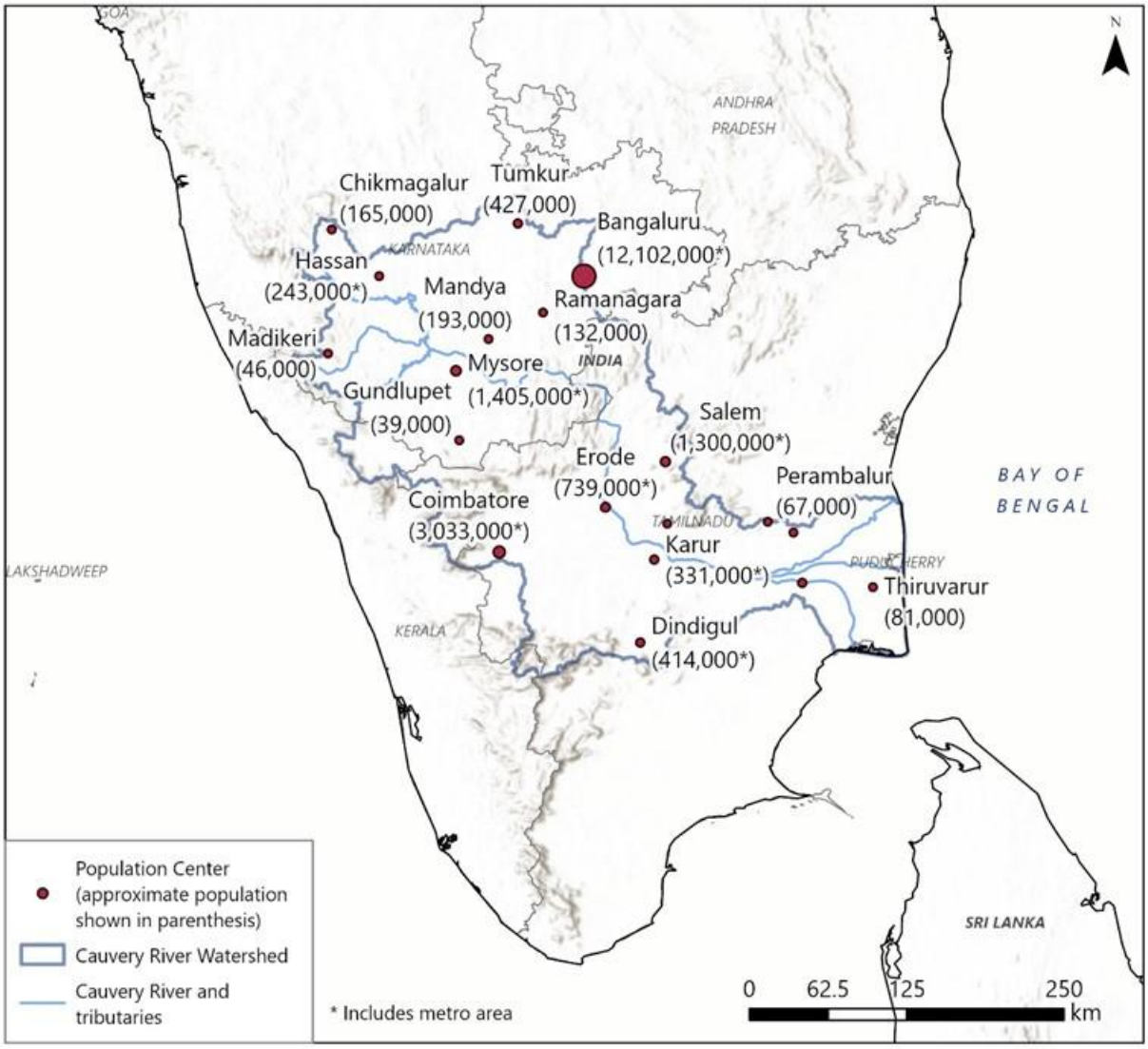

Fig. S4. Cauvery River watershed with population centres. The India populations are based on projected growth rates for 2024. Countries shapefile: Urbano, Ferdinando (2018): Global administrative boundaries. European Commission, Joint Research Centre (JRC) [Dataset] PID: http://data.europa.eu/89h/jrc-10112-10004. Watershed boundaries are from https://indiawris.gov.in/wris/#/geoSpatialData. The Population data is from mohfw.gov.in.

Table S2. Waterbody/Watershed Parameters for Hudson River

The watershed and waterbody parameters for the sub-basins of the Hudson River from the United States Geological Survey (USGS) Database[1] were used in the transport modeling to estimate the surface water TFA concentrations for each sub-basin modeled in this analysis.

Parameter	Sub-Basin 1	Sub-Basin 2	Sub-Basin 3
Waterbody surface area (m^2)	2.87E+08	2.01E+08	2.97E+08
Impervious watershed area receiving deposition (m^2)	1.74E+08	1.38E+09	1.69E+09
Total watershed area receiving deposition (m^2)	7.04E+09	1.39E+10	1.18E+10
Waterbody temperature (K)[1]	288	288	288
Average volumetric flow rate through waterbody (m^3/yr)[2]	5.15E+09	5.80E+09	1.34E+10
Depth of water column (m)[3]	0.91	3.05	10.0
Total suspended solids concentration (mg/L)[4]	4	4	4
Total waterbody depth (m)[5]	0.94	3.08	10.0
Current velocity (m/s)[6]	0.610	0.610	0.610
Average annual precipitation (cm/yr)[7]	110	110	110
Empirical intercept coefficient (unitless)[8]	0.6	0.6	0.6
Average Annual surface runoff from pervious areas (cm/year)[7]	52.5	52.5	52.5
Average annual irrigation (cm/year)[9]	0.981	0.495	0.585
Average annual evapotranspiration (cm/year)[10]	9.13	9.13	27.4
Assumed infiltration (cm/year)[11]	49.4	48.9	30.7

Sources/Notes:

cm: Centimeter
cm/year: Centimeter per year
g/cm^3: Gram per cubic centimeter
g/cm/s: Gram per centimeter-second
K: Kelvin
m: Meter
m/s: Meter per second
mL/cm^3: Milliliter per cubic centimeter
USEPA: United States Environmental Protection Agency
USLE: Universal Soil Loss Equation

[1] USGS Data Statistics
[2] USGS Data at Multiple Gauges: Basin 1: 5,765 cfs (USGS data - several gages), Basin 2 (average of: Mohawk River at Amsterdam:6,000 cfs, Hudson River at Mecahnicaville (7,000 cfs)}; Basin 3 (Middle): 15,000 cfs (USGS gage at Green Island, NY)
[3] Hudson River Nautical Chart: https://usa.fishermap.org/depth-map/hudson-river/
[4] Average TSS from several sampling sites (Hudson River Water Column Concentration Analysis, Malcolm Pirnie/TAMS-Earth-Tec, 2003)
[5] Water depth plus 3-cm of sediment
[6] USGS data at Albany, Mohawk River at Freeman's Bridge
[7] USGS Hudson River Basin National Water Quality Assessment: https://ny.water.usgs.gov/projects/hdsn/fctsht/su.html#:~:text=Average%20annual%20precipitation%20in%20the,southern%20ends%20of%20the%20basin.
[8] United States Environmental Protection Agency (USEPA). 2005. Human Health Risk Assessment Protocol for Hazardous Waste Combustion Facilities, Final EPA530-R-05-006:Solid Waste and Emergency Response, Washington, D.C. September.
[9] USGS Water Use Data for New York: https://waterdata.usgs.gov/ny/nwis/water_use?format=html_table&rdb_compression=file&wu_area=State+Total&wu_year=2015&wu_category=IT&wu_category_nms=Irrigation%252C%2BTotal

[1] https://water.usgs.gov/wsc/watershed_finder.html

[10] National Weather Service Interactive Forecast Tool: https://www.weather.gov/ict/Evapotranspiration
[11] Infiltration was calculated using the following equation: I = (P+I-OR-Ev)

Table S3. Watershed and Waterbody Parameters for Rhine River

The watershed and waterbody parameters for each of the sub-basins of the Rhine River obtained from the EU-Hydro River Network Database[2] were used in the transport modeling to estimate the surface water TFA concentrations for each sub-basin modeled in this analysis.

Parameter	Sub-Basin 1	Sub-Basin 2	Sub-Basin 3	Sub-Basin 4	Sub-Basin 5	Sub-Basin 6
Waterbody surface area (m^2)	2.88E+07	2.74E+07	1.85E+08	1.18E+08	2.13E+08	4.78E+07
Impervious watershed area receiving deposition (m^2)	5.89E+08	6.93E+08	4.06E+09	2.59E+09	2.88E+09	1.85E+09
Total watershed area receiving deposition (m^2)	1.59E+10	1.76E+10	6.49E+10	3.98E+10	2.54E+10	2.53E+10
Waterbody temperature (K)	287	287	287	287	287	287
Average volumetric flow rate through waterbody (m^3/yr)	7.73E+09	3.43E+10	7.88E+10	7.88E+10	9.15E+10	9.15E+10
Depth of water column (m)	4.0	4.0	5.0	7.0	6.0	6.0
Total suspended solids concentration (mg/L)	134.4	14.8	18.9	25.7	28.7	29.4
Total waterbody depth (m)[1]	4.0	4.0	5.0	7.0	6.0	6.0
Current velocity (m/s)	1.50	1.5	1	1.8	1.65	1.5
Average annual precipitation (cm/yr)	2,500	2,000	750	700	650	850
Empirical intercept coefficient (unitless)[2]	0.6	0.6	0.6	0.6	0.6	0.6
Average annual surface runoff from pervious areas (cm/year)	28.6	28.6	28.6	28.6	28.6	28.6
Average annual irrigation (cm/year)	20	20	20	20	20	20
Average annual evapotranspiration (cm/year)	55	55	55	55	55	55
Ambient air temperature (K)	284	284	284	284	284	284
Bed sediment porosity (unitless)	0.225	0.225	0.225	0.225	0.225	0.225
Average annual wind speed (m/s)	6.5	6.5	6.5	6.5	6.5	6.5

Sources/Notes:
cm: Centimeter m: Meter
cm/year: Centimeter per year m/s: Meter per second
g/cm^3: Gram per cubic centimeter mL/cm^3: Milliliter per cubic centimeter
g/cm/s: Gram per centimeter-second USEPA: United States Environmental Protection Agency
K: Kelvin USLE: Universal Soil Loss Equation
[1] Depth of water column plus 0.03 m. [2] United States Environmental Protection Agency (USEPA). 2005. Human Health Risk Assessment Protocol for Hazardous Waste Combustion Facilities, Final EPA530-R-05-006:Solid Waste and Emergency Response, Washington, D.C. September.

[2] https://land.copernicus.eu/imagery-in-situ/eu-hydro/eu-hydro-river-network-database?tab=download

Table S4. Watershed and Waterbody Parameters for Cauvery River

The watershed and waterbody parameters for each of the sub-basins of the Cauvery River gathered from various Indian governmental sources were used in the transport modeling to estimate the surface water TFA concentrations for each sub-basin modeled in this analysis.

Parameter	Sub-Basin 1	Sub-Basin 2	Sub-Basin 3
Waterbody surface area (m^2)[1]	3.77E+08	1.75E+09	5.57E+08
Impervious watershed area receiving deposition (m^2)[2]	2.19E+08	1.72E+09	8.69E+08
Total watershed area receiving deposition (m^2)[3]	1.10E+10	5.73E+10	1.74E+10
Waterbody temperature (K)[4]	296	304	304
Average volumetric flow rate through waterbody (m^3/yr)[5]	9.48E+08	3.87E+09	6.18E+09
Depth of water column (m)[6]	10	5	5
Total suspended solids concentration (mg/L)[7]	11.35	11.35	15.69
Total waterbody depth (m)	10.03	5.03	5.03
Current velocity (m/s)[8]	1	1	1
Average annual precipitation (cm/yr)[5]	126.4	89.9	96.4
Empirical intercept coefficient (unitless)[9]	0.6	0.6	0.6
Average Annual surface runoff from pervious areas (cm/year)[10]	8.65	6.76	35.6
Average annual irrigation (cm/year)[11]	11.63	5.94	0
Average annual evapotranspiration (cm/year)[12]	3.7	3.7	3.7
Assumed infiltration (cm/year)[13]	125.7	85.3	57.1

Sources/Notes:

cm: Centimeter
m: Meter
cm/year: Centimeter per year
m/s: Meter per second
g/cm^3: Gram per cubic centimeter
mL/cm^3: Milliliter per cubic centimeter
g/cm/s: Gram per centimeter-second
USEPA: United States Environmental Protection Agency
K: Kelvin
USLE: Universal Soil Loss Equation

[1] Water Bodies Information System (nrsc.gov.in)： https://bhuvan-wbis.nrsc.gov.in/#!/map
[2] Cauvery Basin Report (2014)
[3] Cauvery Basin Report (2014), Government of India, Central Water Commission, Ministry of Water Resources and National Remote Sensing Center, ISRO Department of Space, Government of India
[4] Water Quality Data Monitoring, 2021: https://cpcb.nic.in/wqm/2021/WQuality_River-Data-2021.pdf
[5] India Water Resources Information System: https://indiawris.gov.in/wris/#/DataDownload
[6] Estimated from water level data at different gages along river (note: significant influence of dams and reservoirs) https://indiawris.gov.in/wris/#/RiverMonitoring
[7] Annual data for National Water Monitoring Project-April 2021 to March 2022
[8] Flood Inundation Mapping of Cauvery River using HEC-RAS and GIS, Sathya and Thampi, in R. M. Singh et. Al. (eds.) Advances in Civil Engineering, page 83.
[9] United States Environmental Protection Agency (USEPA). 2005. Human Health Risk Assessment Protocol for Hazardous Waste Combustion Facilities, Final EPA530-R-05-006:Solid Waste and Emergency Response, Washington, D.C. September.
[10] Cauvery Basin Report (2014), Government of India, Central Water Commission, Ministry of Water Resources and National Remote Sensing Center, ISRO Department of Space, Government of India
[11] Data from Graph
[12] Study of Evapotranspiration in Cauvery River Catchment Area: https://www.linkedin.com/pulse/study-evaporotranspiration-cauvery-river-catchment-area-sunkara/
[13] Infiltration was calculated using the following equation: I = (P+I-OR-Ev)

Table S5. Other Modeling Parameters for Hudson River

Other modeling parameters used in transport modeling to predict the TFA concentrations in soil and surface water from air deposition in the Hudson River basin. Most parameters are based on default recommended values from the HHRAP Guidance.

Parameter	Unit	Symbol	Value	Source
Time period of deposition	year	tD	30	Site-specific
Time period at the beginning of deposition	year	T_1	0	USEPA 2005
Soil mixing zone depth	cm	Z_s	2	USEPA 2005
Soil bulk density	g/cm^3	BD	1.5	USEPA 2005
Loss Constant Due to Soil Erosion	$year^{-1}$	kse	0	USEPA 2005
Soil volumetric water content	mL/cm^3	θ_{sw}	0.2	USEPA 2005
Ambient air temperature	K	T_a	282	Site-specific
Solids particle density	g/cm^3	ρ_s	2.7	USEPA 2005
USLE rainfall (or erosivity) factor [1,2,3,4]	$year^{-1}$	RF	52.7	Region-specific
USLE erodibility factor	ton/acre	K	0.36	USEPA 2005
USLE length-slope factor	unitless	LS	1.5	USEPA 2005
USLE cover management factor	unitless	C	1	USEPA 2005
USLE supporting practice factor	unitless	PF	1	USEPA 2005
Empirical slope coefficient	unitless	b	0.125	USEPA 2005
Depth of upper benthic sediment layer	m	d_{bs}	0.03	USEPA 2005
Bed sediment concentration	g/cm^3	C_{BS}	1	USEPA 2005
Bed sediment porosity	unitless	θ_{bs}	0.4	Site-specific
Temperature correction factor	unitless	θ	1.026	USEPA 2005
Drag coefficient	unitless	C_d	0.0011	USEPA 2005
Average annual wind speed	m/s	W	5	Site-specific
Density of air	g/cm^3	ρ_a	0.0012	USEPA 2005
Density of water	g/cm^3	ρ_w	1	USEPA 2005
von Karman's constant	unitless	k	0.4	USEPA 2005
Dimensionless viscous sublayer thickness	unitless	λ_z	4	USEPA 2005
Viscosity of water corresponding to water temperature	g/cm/s	μ_w	0.0169	USEPA 2005
Viscosity of air	g/cm/s	μ_a	0.0018	USEPA 2005

Sources/Notes:
cm: Centimeter
cm/year: Centimeter per year
g/cm^3: Gram per cubic centimeter
g/cm/s: Gram per centimeter-second
K: Kelvin
m: Meter
m/s: Meter per second
mL/cm^3: Milliliter per cubic centimeter
USEPA: United States Environmental Protection Agency
USLE: Universal Soil Loss Equation

[1]The average RF of 26 (year-1) in Europe was converted from 450 (MJ mm)/(ha-h-yr) (Estimated from graph from Panos Panagos et al, 2015: Rainfall Erosivity in Europe) divided by 17.02 using the method recommended by USLE (Foster G.R. 1981, and Benavidez R., 2018).
[2] Benavidez R. et al, 2018. A review of the (Revised) Universal Soil Loss Equation ((R)USLE): with a view to increasing its global applicability and improving soil loss estimates
[3] Foster. G.R. et al, 1981. Conversion of the Universal Soil Loss Equation to SI Metric Units.
[4] Panagos et al, 2015. Rainfall Erosivity in Europe.
[5] United States Environmental Protection Agency (USEPA). 2005. Human Health Risk Assessment Protocol for Hazardous Waste Combustion Facilities, Final EPA530-R-05-006:Solid Waste and Emergency Response, Washington, D.C. September.

Table S6. Other Modeling Parameters for Rhine River

Other modeling parameters used in transport modeling to predict the TFA concentrations in soil and surface water from air deposition in the Rhine River basin. Most parameters are based on default recommended values from the HHRAP Guidance.

Parameter	Unit	Symbol	Value	Source
Time period of deposition	year	tD	30	Site-specific
Time period at the beginning of deposition	year	T_1	0	USEPA 2005
Soil mixing zone depth	cm	Z_s	2	USEPA 2005
Soil bulk density	g/cm^3	BD	1.5	USEPA 2005
Loss Constant Due to Soil Erosion	$year^{-1}$	kse	0	USEPA 2005
Soil volumetric water content	mL/cm^3	θ_{sw}	0.2	USEPA 2005
Solids particle density	g/cm^3	ρ_s	2.7	USEPA 2005
USLE rainfall (or erosivity) factor [1,2,3,4]	$year^{-1}$	RF	26.4	Site-specific
USLE erodibility factor	ton/acre	K	0.36	USEPA 2005
USLE length-slope factor	unitless	LS	1.5	USEPA 2005
USLE cover management factor	unitless	C	1	USEPA 2005
USLE supporting practice factor	unitless	PF	1	USEPA 2005
Empirical slope coefficient	unitless	b	0.125	USEPA 2005
Depth of upper benthic sediment layer	m	d_{bs}	0.03	USEPA 2005
Bed sediment concentration	g/cm^3	C_{BS}	1	USEPA 2005
Temperature correction factor	unitless	θ	1.026	USEPA 2005
Drag coefficient	unitless	C_d	0.0011	USEPA 2005
Density of air	g/cm^3	ρ_a	0.0012	USEPA 2005
Density of water	g/cm^3	ρ_w	1	USEPA 2005
von Karman's constant	unitless	k	0.4	USEPA 2005
Dimensionless viscous sublayer thickness	unitless	λ_z	4	USEPA 2005
Viscosity of water corresponding to water temperature	g/cm/s	μ_w	0.0169	USEPA 2005
Viscosity of air	g/cm/s	μ_a	0.00018	USEPA 2005

Sources/Notes:
cm: Centimeter
cm/year: Centimeter per year
g/cm^3: Gram per cubic centimeter
g/cm/s: Gram per centimeter-second
K: Kelvin
m: Meter
m/s: Meter per second
mL/cm^3: Milliliter per cubic centimeter
USEPA: United States Environmental Protection Agency
USLE: Universal Soil Loss Equation

[1]The average RF of 26 (year-1) in Europe was converted from 450 (MJ mm)/(ha-h-yr) (Estimated from graph from Panos Panagos et al, 2015: Rainfall Erosivity in Europe) divided by 17.02 using the method recommended by USLE (Foster G.R. 1981, and Benavidez R., 2018).
[2] Benavidez R. et al, 2018. A review of the (Revised) Universal Soil Loss Equation ((R)USLE): with a view to increasing its global applicability and improving soil loss estimates
[3] Foster. G.R. et al, 1981. Conversion of the Universal Soil Loss Equation to SI Metric Units.
[4] Panagos et al, 2015. Rainfall Erosivity in Europe.
[5] United States Environmental Protection Agency (USEPA). 2005. Human Health Risk Assessment Protocol for Hazardous Waste Combustion Facilities, Final EPA530-R-05-006:Solid Waste and Emergency Response, Washington, D.C. September.

Table S7. Other Modeling Parameters for Cauvery River

Other modeling parameters used in transport modeling to predict the TFA concentrations in soil and surface water from air deposition in the Cauvery River basin. Most parameters are based on default recommended values from the HHRAP Guidance.

Parameter	Unit	Symbol	Value	Source
Time period of deposition	year	tD	30	Site-specific
Time period at the beginning of deposition	year	T_1	0	USEPA 2005
Soil mixing zone depth	cm	Z_s	2	USEPA 2005
Soil bulk density	g/cm^3	BD	1.5	USEPA 2005
Loss Constant Due to Soil Erosion	$year^{-1}$	kse	0	USEPA 2005
Soil volumetric water content	mL/cm^3	θ_{sw}	0.2	USEPA 2005
Solids particle density	g/cm^3	ρ_s	2.7	USEPA 2005
USLE rainfall (or erosivity) factor [1,2,3,4]	$year^{-1}$	RF	351.3	USEPA 2005
USLE erodibility factor	ton/acre	K	0.36	USEPA 2005
USLE length-slope factor	unitless	LS	1.5	USEPA 2005
USLE cover management factor	unitless	C	1	USEPA 2005
USLE supporting practice factor	unitless	PF	1	USEPA 2005
Empirical slope coefficient	unitless	b	0.125	USEPA 2005
Depth of upper benthic sediment layer	m	d_{bs}	0.03	USEPA 2005
Bed sediment concentration	g/cm^3	C_{BS}	1	USEPA 2005
Temperature correction factor	unitless	θ	1.026	USEPA 2005
Drag coefficient	unitless	C_d	0.0011	USEPA 2005
Density of air	g/cm^3	ρ_a	0.0012	USEPA 2005
Density of water	g/cm^3	ρ_w	1	USEPA 2005
von Karman's constant	unitless	k	0.4	USEPA 2005
Dimensionless viscous sublayer thickness	unitless	λ_z	4	USEPA 2005
Viscosity of water corresponding to water temperature	g/cm/s	μ_w	0.0169	USEPA 2005
Viscosity of air	g/cm/s	μ_a	0.00018	USEPA 2005

Sources/Notes:
cm: Centimeter
cm/year: Centimeter per year
g/cm^3: Gram per cubic centimeter
g/cm/s: Gram per centimeter-second
K: Kelvin
m: Meter
m/s: Meter per second
mL/cm^3: Milliliter per cubic centimeter
USEPA: United States Environmental Protection Agency
USLE: Universal Soil Loss Equation

[1]The average RF of 26 (year-1) in Europe was converted from 450 (MJ mm)/(ha-h-yr) (Estimated from graph from Panos Panagos et al, 2015: Rainfall Erosivity in Europe) divided by 17.02 using the method recommended by USLE (Foster G.R. 1981, and Benavidez R., 2018).

[2] Benavidez R. et al, 2018. A review of the (Revised) Universal Soil Loss Equation ((R)USLE): with a view to increasing its global applicability and improving soil loss estimates
[3] Foster. G.R. et al, 1981. Conversion of the Universal Soil Loss Equation to SI Metric Units.
[4] Panagos et al, 2015. Rainfall Erosivity in Europe.
[5] United States Environmental Protection Agency (USEPA). 2005. Human Health Risk Assessment Protocol for Hazardous Waste Combustion Facilities, Final EPA530-R-05-006:Solid Waste and Emergency Response, Washington, D.C. September.

Section S1: Parameter uncertainties associated with the Watershed/Catchment Model

Some default modeling parameters are used when site-specific data are not available, and these recommended values typically reflect average conditions in the respective watershed area and may not accurately represent site-specific water body conditions. These values may be more appropriate for some locations or regions, and less so for others. However, the ranges of these default parameters are either relatively narrow or the impact on the modeling results is insignificant. Other parameters were reasonably estimated based on generally available information for the sub-basins of each River. Other variables were reasonably estimated based on generally available information for each modeled river.

For example, the recommended default value for the empirical intercept coefficient has relatively small impact on the modeling results. This parameter is an estimated average value that is based on studies of sediment yields from various watersheds. Therefore, the default value may not accurately represent site-specific watershed conditions. As a result, using the default value may slightly under- or over-estimate the TFA concentrations in surface water and sediment.

The key factors that have significant impacts on the modeling results include TFA deposition rates, impervious area in the watershed, volumetric flow rate, and total infiltrations, as discussed below:

- The TFA concentration in surface water increases significantly with the increase of the watershed area; the impact on the TFA concentration in surface water due to the percentage change in the watershed area is more significant than the change in the water body because the contribution of the TFA load from the soil in the watershed is much larger than the direct deposition from the air on the water body. The watershed area estimates are based on sub-basin-specific measurements in GIS based on the available watershed data from USGS, the EU-Hydro River Network Database, and the Indian Government. The uncertainty associated with this parameter is considered low.
- The modeled TFA concentration in surface water decreases significantly when the river flow rate increases. The availability of the volumetric flow rate data at gages, the spatial coverage, and the specific gage location (on the main river vs. located at less relevant locations) all have impacts on the estimated of the volumetric flow rate and the subsequent modeled TFA concentrations in surface water. The uncertainty associated with this parameter increases when the flow rate data from gages on the mainstream of the river are limited (e.g., very few gage locations on the mainstream of the river, the spatial coverage is poor, or the measurements are limited).
- The infiltration in each sub-basin is determined by precipitation, irrigation, run-off, and average evapotranspiration. The precipitation data, in general, has less uncertainty, while the irrigation, run-off, and average evapotranspiration are often based on estimates for a relatively large region and may not be accurate for each sub-basin. The modeled TFA concentration in surface water concentration decreases significantly when total infiltration increases (assuming the same deposition rate), primarily due to increased loss of TFA in soil by leaching which results in lower TFA concentrations in soil (note that the contribution of TFA to surface water from groundwater discharge is not simulated in this model).

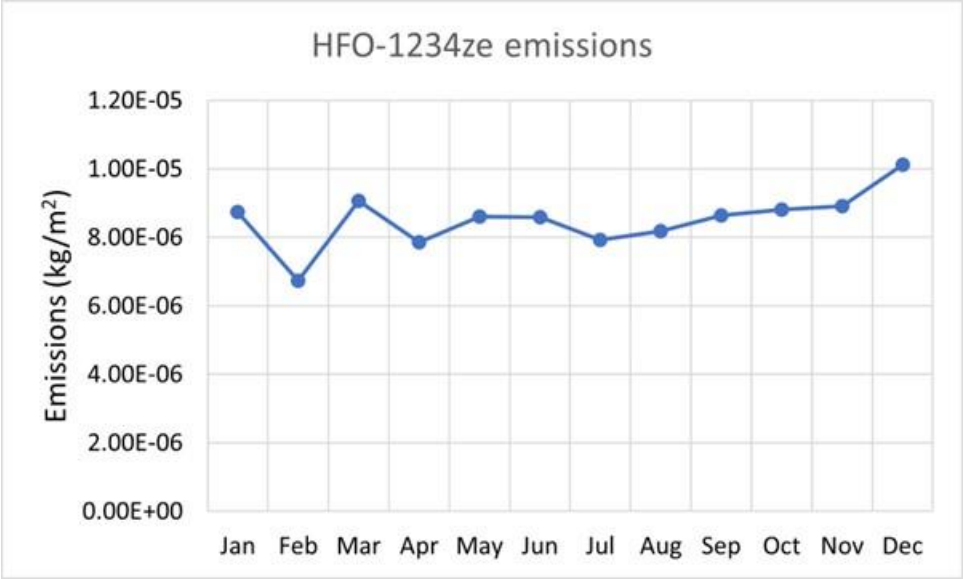

Fig. S5. Global monthly variation in HFO-1234ze emissions(E) in GEOS-Chem

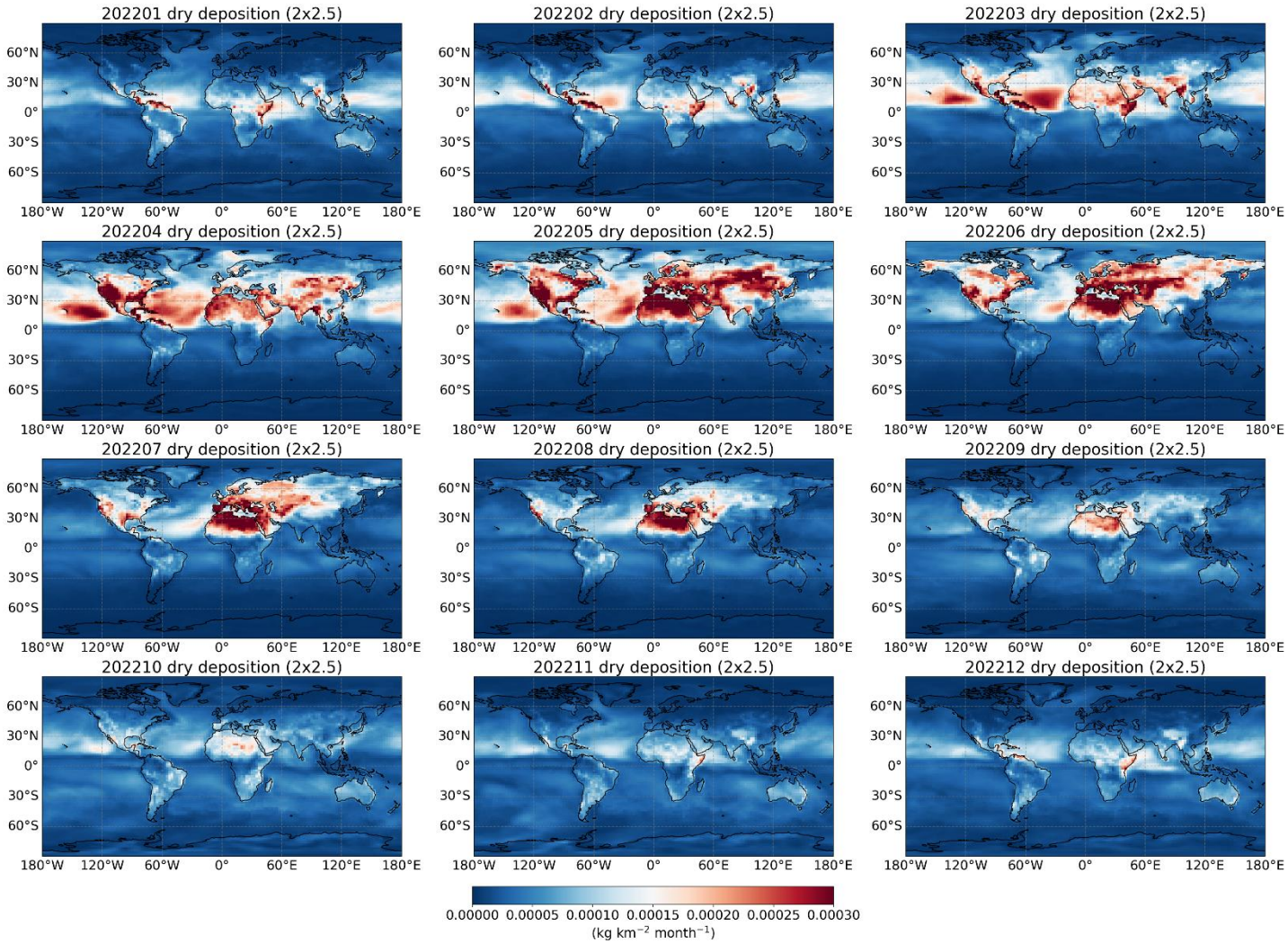

Fig. S6. Global monthly variation in dry deposition of TFA at 2×2.5° resolution. *Title*: 202201 = January of 2022.

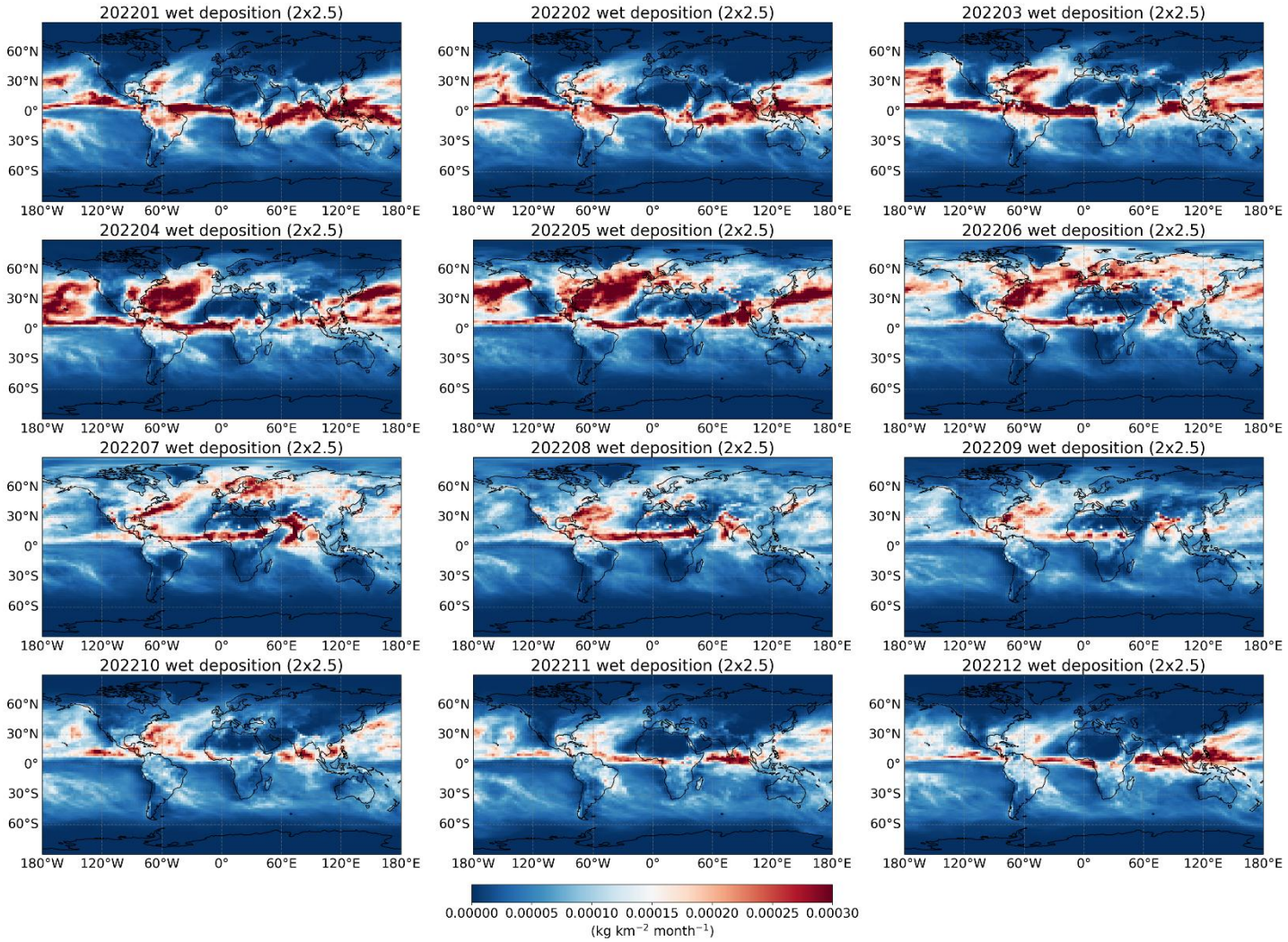

Fig. S7. Global monthly variation in wet deposition of TFA at 2×2.5° resolution**.** *Title***:** 202201 = January of 2022

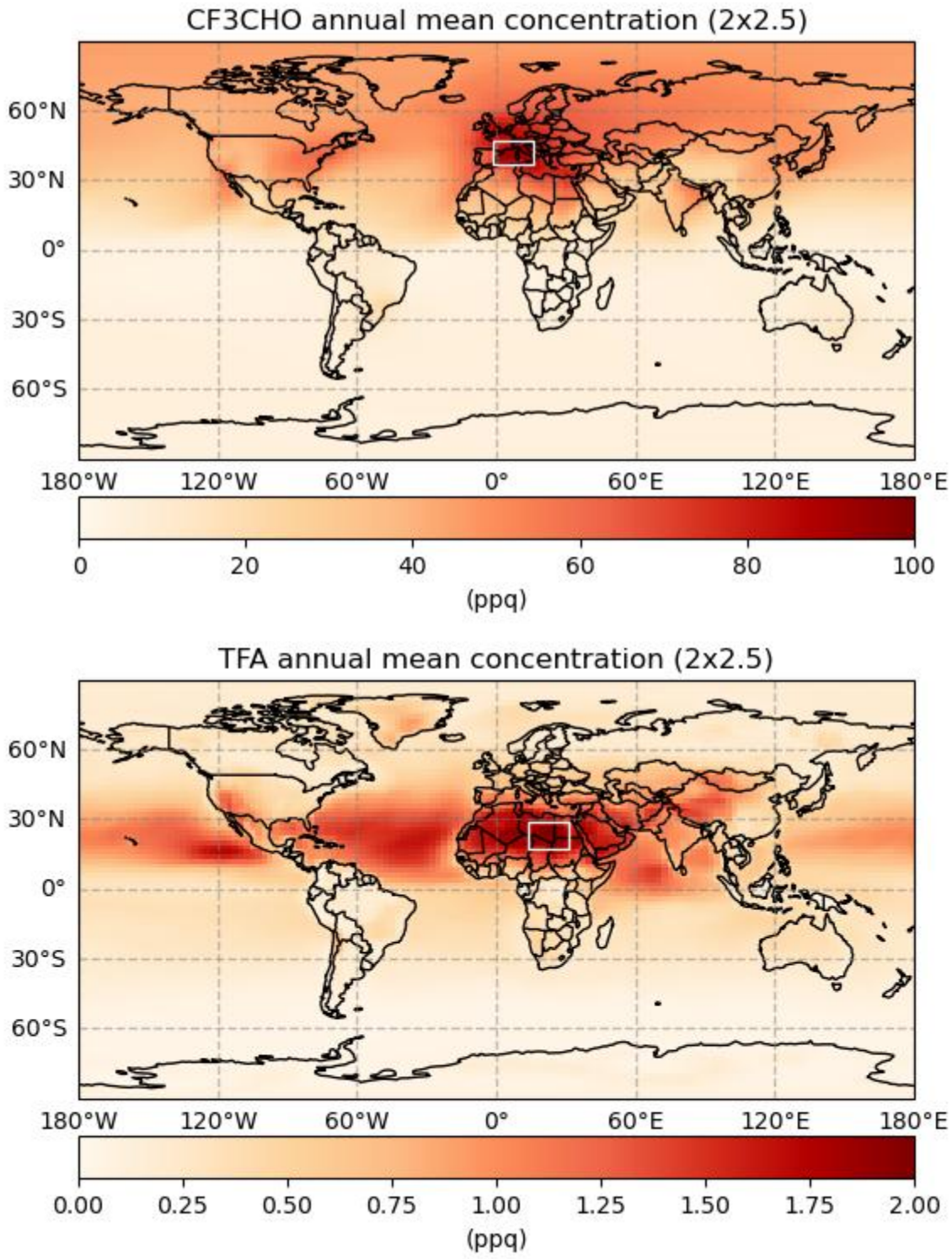

Fig. S8: Annual mean concentrations of trifluoroacetaldehyde (CF_3CHO) and trifluoroacetic acid (TFA) at 2×2.5° resolution. The white rectangle marks two regions: *1*) high CF_3CHO in the northern temperate region with high pMDI sales and *2*) high TFA in the tropical region with low (or no) pMDI sale.

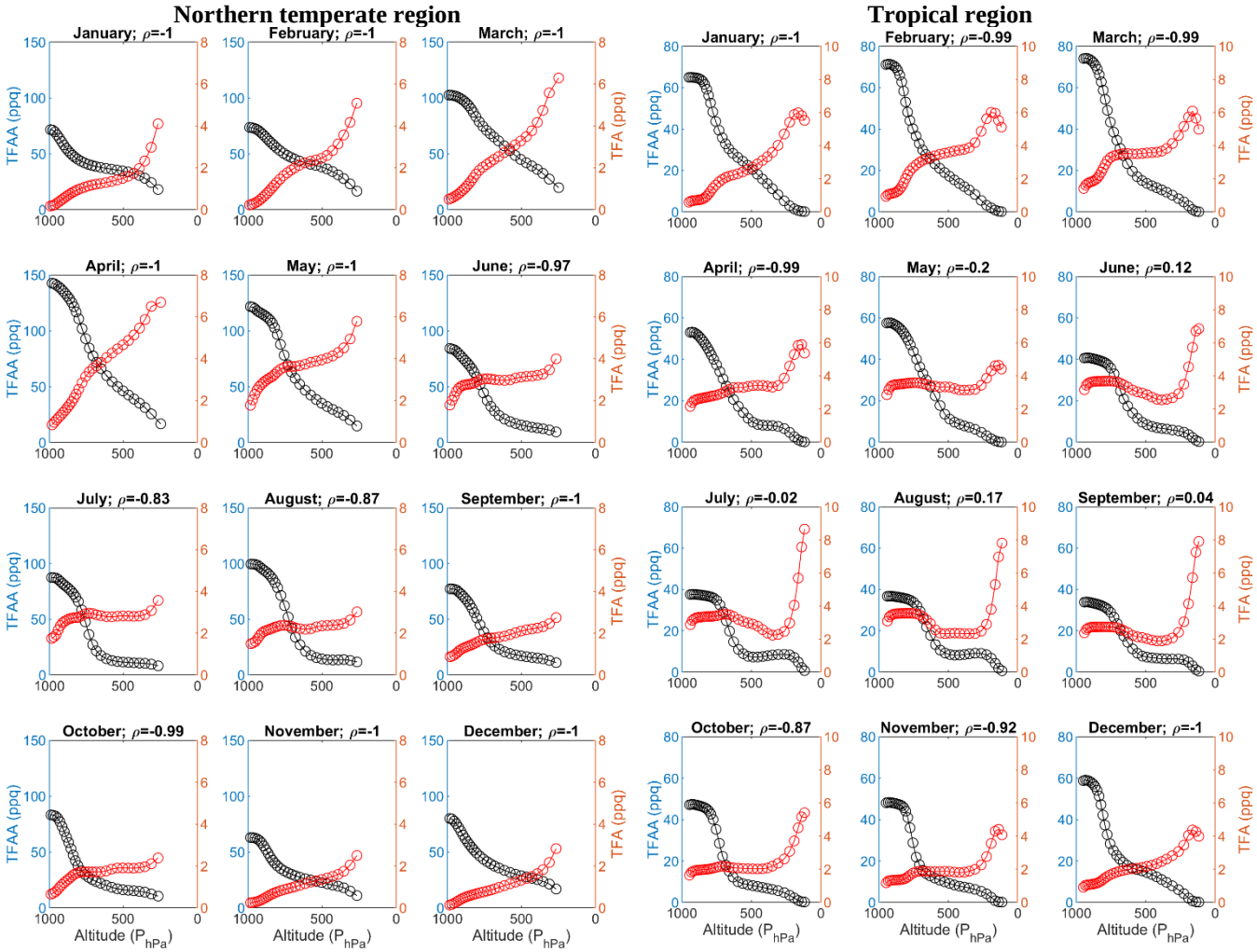

Fig. S9: Spearman Correlation (ρ) between trifluoroacetic aldehyde (TFAA) and trifluoroacetic acid (TFA) in two identified regions of Europe and Africa (Figure S5). This analysis confirms that hydroxyl radical (OH) route of TFAA is the predominant route of TFA formation. Although, under some environmental conditions, channels other than OH route may contribute to formation of gas-phase TFA.

Section S2: Identify the primary precursors of TFA formation in the atmosphere

To this end, we examined concentrations of various species in 4°×5° simulation (spin-up #11) at the surface for reactions that produce and remove TFA in the atmosphere, which are presented below for the convenience of the reader. Spin-up simulations were performed at 4°×5° resolution for computational efficiency; therefore, the results shown are approximate. Aside from differences in spatial resolution, the overall chemical behavior is expected to be consistent with the higher-resolution (2°×2.5°) simulation.

- Reaction of HFO (CF_3CHCHF) with hydroxyl radical (OH)
  - $CF_3CHCHF + OH \rightarrow CF_3CH(OH)CH(OO)F$ (1)
  - $CF_3CH(OH)CH(OO)F + NO \rightarrow CF_3CHO + HCOF + HO_2 + NO_2$ (2a)
  - $CF_3CH(OH)CH(OO)F + HO_2 \rightarrow CF_3CH(OH)C(O)F$ (2b)
  - (2a) is faster than (2b) – lead to higher CF_3CHO (Figure S6d) concentration compared to $CF_3CH(OH)C(O)F$ (Figure S6c).
- Spatial pattern of CF_3CHO follows the location of HFO-1234ze emissions (Figure S6a).

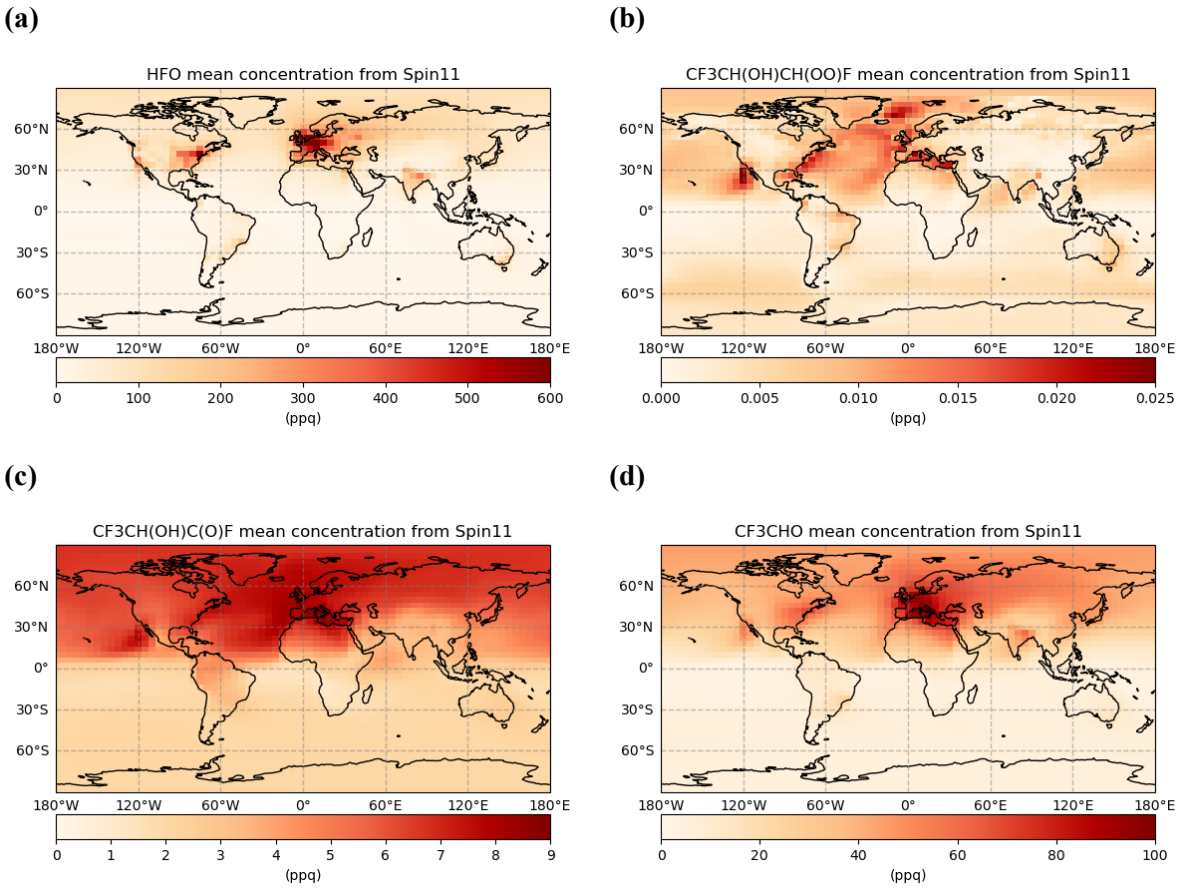

Figure S10. Annual mean concentrations of (a) CF_3CHCHF, (b) $CF_3CH(OH)CH(OO)F$, (c) $CF_3CH(OH)C(O)F$, and (d) CF_3CHO at the surface from 4°×5° simulation.

- CF_3CHO can degrade via photolysis (major route) and reaction with OH and HO_2 (Reactions 3a and 3b).
    - $CF_3CHO + OH\ (+O_2) \rightarrow CF_3C(O)O_2$ (3a)
    - $CF_3CHO + HO_2 \rightarrow CF_3CH(OH)O_2$ (3b)
    - Reaction (3a) is faster than reaction (3b) by ~3 orders of magnitude – lead to more $CF_3C(O)O_2$ (Figure S7a) concentrations compared to $CF_3CH(OH)O_2$ (Figure Ss7b).

(a) **(b)**

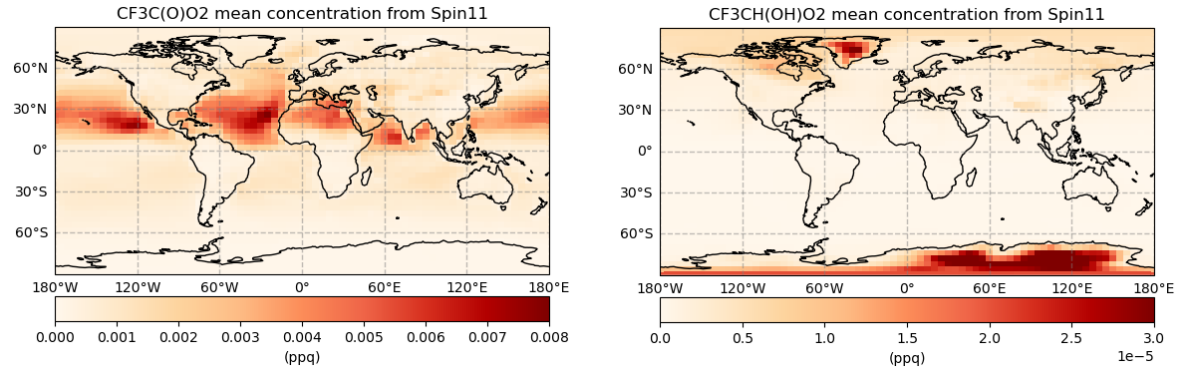

Figure S11. Annual mean concentrations of (a) $CF_3C(O)O_2$ and (b) $CF_3CH(OH)O_2$ at the surface from 4°×5° simulation.

- Other pathways leading to the formation of $CF_3C(O)O_2$ are the following:
    - $CF_3C(O)OONO_2 \rightarrow CF_3C(O)O_2 + NO_2$ (4a)
    - $CF_3C(O)OONO_2 + h\nu \rightarrow 0.5*CF_3C(O)O_2 + 0.5*NO_2 + 0.5*CF_3C(O)O + 0.5*NO_3$ (4b)
    - $CF_3C(O)C(O)F + h\nu \rightarrow CF_3CO_3$ (4c)

Note that 4a, 4b, and 4c are minor reactions compared to 3a.

- TFA formation pathways:
    - $CF_3C(O)O_2 + HO_2 \rightarrow CF_3COOH + O_3$ (5a)
    - $CF_3C(O)O_2 + CH_3O_2 \rightarrow CF_3COOH$ (5b)

Reaction (5a) is faster than (5b) and concentrations of HO_2 are higher than CH_3O_2.

- TFA removal pathway:
    - $CF_3C(O)OH + OH \rightarrow CF_3C(O)O + H$ (6)

Figure S8 shows the spatial pattern of annual mean concentrations of OH and HO2. They are generally high in the -30 to +30 latitudes.

(a) (b)

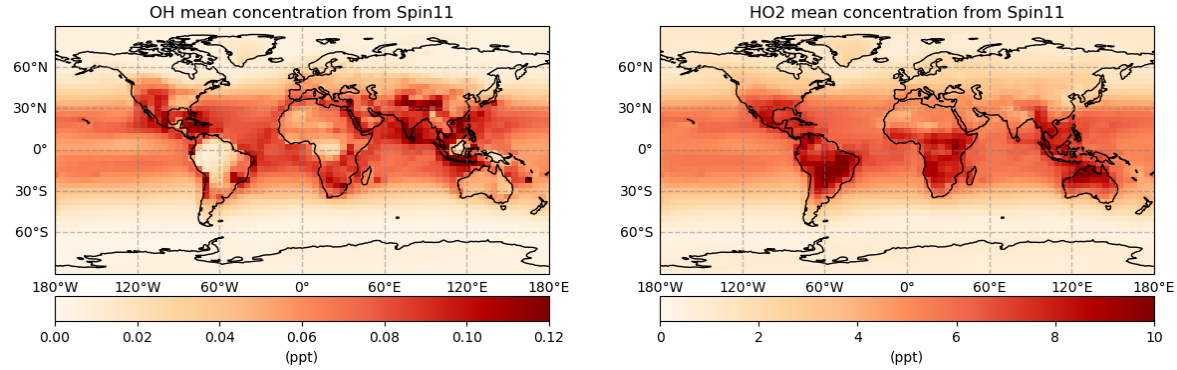

Figure S12. Annual mean concentration of (a) OH and (b) HO_2 concentration at the surface from 4°×5° simulation.

- Calculated the ratio ([HO_2] x [$CF_3C(O)O_2$])/[OH] (Reactions 5a and 6; Figure S9b), which accounts for the species leading to the formation and removal of TFA (CF_3COOH) in the atmosphere.

(a) (b)

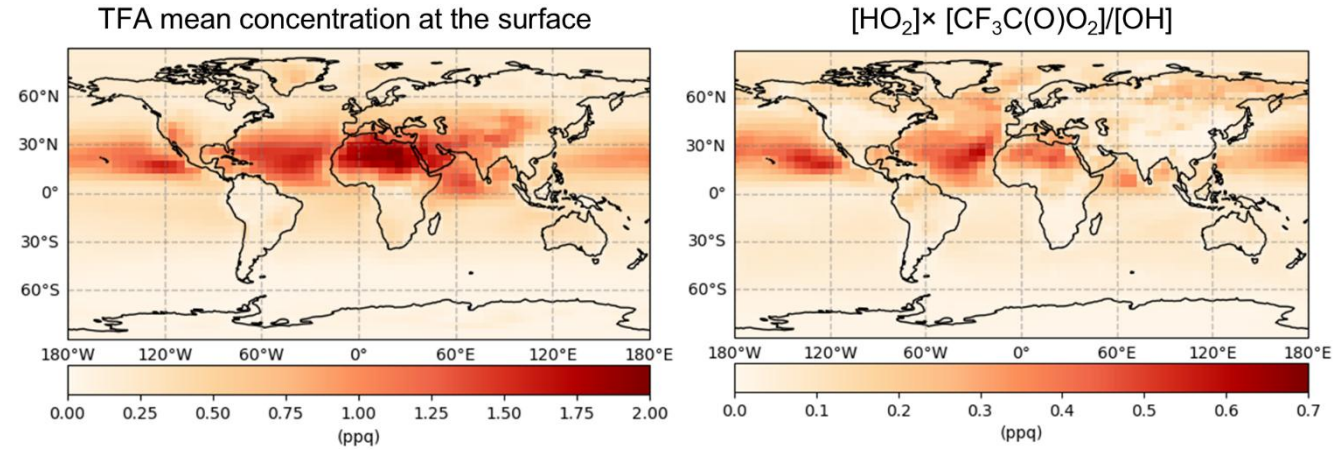

Figure S13. Annual mean concentration of (a) TFA concentration and (b) ([HO_2] x [$CF_3C(O)O_2$])/[OH] at the surface from 4°×5° simulation.

The availability of $CF_3C(O)O_2$, HO_2, and OH controls the spatial pattern of TFA (gas-phase) at the surface. The spatial pattern of the ratio of ([HO_2] × [$CF_3C(O)O_2$])/[OH] generally matches the spatial pattern of TFA (gas-phase) concentration. Moreover, since spatial pattern of the ratio (Fig. S13b) generally matches that of CF3C(O)O2 (Fig. S11a), we can postulate that the primary precursor of TFA formation due to oxidation of HFO-1234ze(E) in the atmosphere is $CF_3C(O)O_2$. Note that Figure S13 has been shown here for completeness of this analysis and is same as Figure 5 of the manuscript.

Section S3: Monthly TFA rainwater concentrations

TFA rainwater concentrations were estimated by dividing the monthly modeled wet deposition flux (Fig. S7) by precipitation. The global precipitation values are from the MERRA-2 reanalysis, which provides assimilated meteorological fields that drive the GEOS-Chem model. These are both spatially and temporally varying.

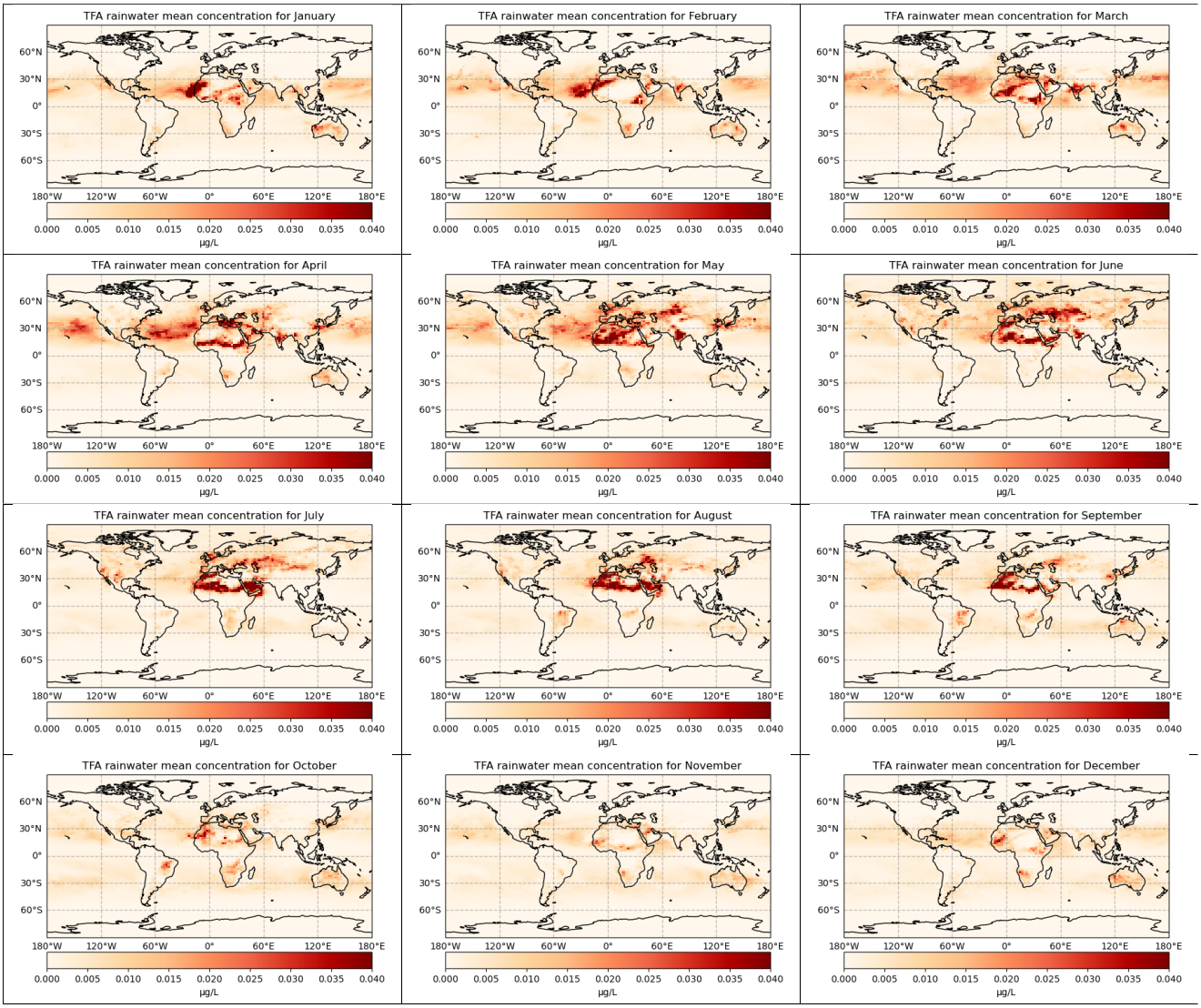

Figure S14. Estimated monthly TFA in rainwater due to future pMDIs releasing HFO-1234ze(E) in the environment. From visual inspection, TFA in rainwater is relatively higher in April-September as compared to rest of the months.

Supplemental Data:

Author analysis based on IQVIA MIDAS® monthly volume sales data for period January 2022 to December 2022 reflecting estimates of real-world activity.

	HFO released from pMDI usage per month (Gg month^{-1})											
Country	**Jan**	**Feb**	**Mar**	**Apr**	**May**	**Jun**	**Jul**	**Aug**	**Sep**	**Oct**	**Nov**	**Dec**
Algeria	0.0090	0.0041	0.0045	0.0030	0.0044	0.0064	0.0035	0.0069	0.0073	0.0076	0.0044	0.0048
Argentian	0.0042	0.0032	0.0052	0.0052	0.0065	0.0063	0.0058	0.0052	0.0050	0.0048	0.0043	0.0039
Australia	0.0275	0.0118	0.0183	0.0206	0.0263	0.0269	0.0291	0.0286	0.0230	0.0261	0.0252	0.0269
Austria	0.0016	0.0015	0.0022	0.0019	0.0019	0.0019	0.0019	0.0017	0.0019	0.0021	0.0022	0.0028
Belgium	0.0018	0.0016	0.0023	0.0019	0.0022	0.0023	0.0019	0.0016	0.0017	0.0019	0.0020	0.0029
Brazil	0.0247	0.0184	0.0282	0.0246	0.0331	0.0357	0.0329	0.0309	0.0294	0.0272	0.0252	0.0241
Bulgaria	0.0008	0.0007	0.0008	0.0008	0.0008	0.0008	0.0008	0.0009	0.0008	0.0009	0.0008	0.0009
Canda	0.0118	0.0085	0.0112	0.0107	0.0126	0.0118	0.0111	0.0115	0.0118	0.0143	0.0158	0.0149
Central America	0.0010	0.0008	0.0008	0.0007	0.0008	0.0009	0.0009	0.0008	0.0009	0.0010	0.0010	0.0010
Chile	0.0019	0.0016	0.0019	0.0019	0.0030	0.0032	0.0026	0.0025	0.0022	0.0023	0.0025	0.0023
China	0.0096	0.0039	0.0069	0.0066	0.0057	0.0066	0.0070	0.0073	0.0077	0.0056	0.0065	0.0066
Colombia	0.0035	0.0022	0.0028	0.0028	0.0028	0.0034	0.0032	0.0032	0.0027	0.0027	0.0033	0.0029
Croatia	0.0005	0.0004	0.0006	0.0005	0.0005	0.0005	0.0004	0.0004	0.0005	0.0005	0.0005	0.0006
Czech	0.0023	0.0021	0.0028	0.0024	0.0028	0.0025	0.0019	0.0022	0.0023	0.0023	0.0023	0.0025
Denmark	0.0008	0.0007	0.0009	0.0008	0.0009	0.0008	0.0009	0.0008	0.0008	0.0009	0.0009	0.0010
Egypt	0.0062	0.0064	0.0046	0.0075	0.0056	0.0037	0.0058	0.0071	0.0057	0.0091	0.0083	0.0091
Finland	0.0008	0.0008	0.0012	0.0010	0.0011	0.0010	0.0009	0.0011	0.0011	0.0012	0.0012	0.0017
France	0.0166	0.0132	0.0185	0.0166	0.0167	0.0162	0.0156	0.0133	0.0167	0.0196	0.0192	0.0224
Germany	0.0067	0.0060	0.0083	0.0071	0.0082	0.0074	0.0075	0.0066	0.0072	0.0079	0.0090	0.0104
Greece	0.0026	0.0020	0.0033	0.0026	0.0024	0.0021	0.0021	0.0017	0.0020	0.0030	0.0036	0.0050
Hungary	0.0014	0.0013	0.0017	0.0014	0.0014	0.0014	0.0012	0.0013	0.0014	0.0015	0.0015	0.0019
India	0.0417	0.0308	0.0343	0.0362	0.0350	0.0328	0.0348	0.0367	0.0371	0.0394	0.0439	0.0463
Italy	0.0074	0.0063	0.0084	0.0080	0.0087	0.0070	0.0069	0.0063	0.0067	0.0076	0.0078	0.0087
Japan	0.0063	0.0054	0.0065	0.0075	0.0069	0.0067	0.0065	0.0063	0.0063	0.0068	0.0067	0.0079
Jordan	0.0003	0.0003	0.0003	0.0004	0.0003	0.0003	0.0003	0.0004	0.0003	0.0004	0.0004	0.0004
Kazakhstan	0.0009	0.0015	0.0013	0.0014	0.0011	0.0010	0.0015	0.0012	0.0012	0.0014	0.0010	0.0010
Korea	0.0011	0.0009	0.0013	0.0012	0.0012	0.0011	0.0011	0.0011	0.0011	0.0012	0.0012	0.0012
Kuwait	0.0005	0.0002	0.0002	0.0002	0.0002	0.0001	0.0002	0.0002	0.0003	0.0004	0.0002	0.0001

Lebanon	0.0003	0.0002	0.0003	0.0002	0.0002	0.0003	0.0003	0.0003	0.0001	0.0001	0.0001	0.0005
Mexico	0.0038	0.0022	0.0022	0.0019	0.0022	0.0023	0.0027	0.0022	0.0023	0.0030	0.0032	0.0035
Morocco	0.0040	0.0026	0.0044	0.0033	0.0032	0.0035	0.0030	0.0030	0.0039	0.0037	0.0033	0.0033
Netherlands	0.0051	0.0045	0.0061	0.0053	0.0060	0.0057	0.0056	0.0055	0.0053	0.0056	0.0059	0.0068
Norway	0.0009	0.0009	0.0012	0.0011	0.0011	0.0012	0.0010	0.0011	0.0012	0.0012	0.0013	0.0015
Philippines	0.0025	0.0025	0.0026	0.0015	0.0017	0.0023	0.0017	0.0030	0.0027	0.0022	0.0028	0.0026
Poland	0.0053	0.0044	0.0061	0.0052	0.0052	0.0045	0.0047	0.0043	0.0050	0.0052	0.0049	0.0061
Portugal	0.0020	0.0017	0.0022	0.0019	0.0022	0.0019	0.0018	0.0018	0.0018	0.0025	0.0028	0.0030
Romania	0.0020	0.0016	0.0020	0.0019	0.0018	0.0017	0.0018	0.0020	0.0019	0.0020	0.0021	0.0022
Russia	0.0152	0.0133	0.0222	0.0130	0.0140	0.0131	0.0138	0.0148	0.0150	0.0141	0.0136	0.0157
Saudi Arabia	0.0037	0.0032	0.0034	0.0026	0.0027	0.0039	0.0009	0.0029	0.0032	0.0051	0.0038	0.0042
Serbia	0.0011	0.0010	0.0013	0.0011	0.0011	0.0011	0.0011	0.0012	0.0011	0.0011	0.0010	0.0012
South Africa	0.0030	0.0034	0.0047	0.0032	0.0044	0.0035	0.0036	0.0035	0.0045	0.0032	0.0033	0.0040
Spain	0.0121	0.0100	0.0132	0.0124	0.0139	0.0114	0.0108	0.0100	0.0106	0.0127	0.0136	0.0156
Sweden	0.0009	0.0009	0.0012	0.0010	0.0012	0.0011	0.0008	0.0009	0.0011	0.0012	0.0012	0.0013
Switzerland	0.0008	0.0007	0.0010	0.0009	0.0010	0.0009	0.0008	0.0007	0.0008	0.0009	0.0011	0.0013
Taiwan	0.0008	0.0006	0.0008	0.0007	0.0008	0.0008	0.0008	0.0008	0.0008	0.0008	0.0008	0.0009
Tunisia	0.0024	0.0018	0.0020	0.0018	0.0021	0.0019	0.0015	0.0017	0.0019	0.0021	0.0023	0.0023
Turkey	0.0119	0.0085	0.0110	0.0098	0.0105	0.0124	0.0059	0.0102	0.0096	0.0112	0.0111	0.0111
UAE	0.0007	0.0005	0.0005	0.0004	0.0005	0.0005	0.0005	0.0006	0.0005	0.0007	0.0008	0.0006
UK	0.0451	0.0375	0.0483	0.0426	0.0467	0.0435	0.0445	0.0447	0.0439	0.0456	0.0461	0.0493
Ukraine	0.0021	0.0019	0.0032	0.0022	0.0014	0.0012	0.0013	0.0015	0.0016	0.0018	0.0015	0.0017
US	0.0871	0.0687	0.0962	0.0744	0.0830	0.0922	0.0716	0.0776	0.0980	0.0818	0.0845	0.1139

*calculations based on Hospital usage only

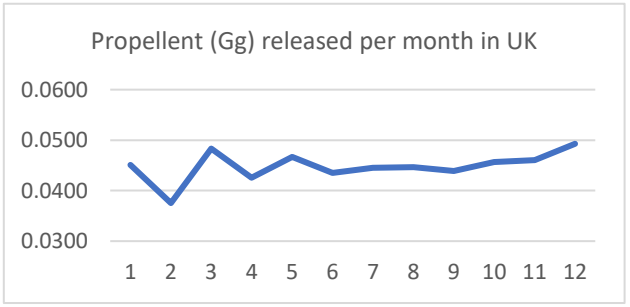

Inhaler sales and usage based estimates of propellant released per month in UK. See calculation process below.

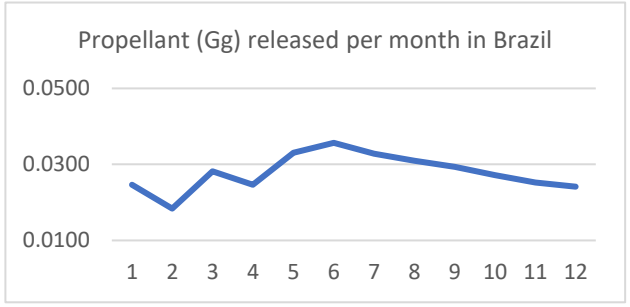

Inhaler sales and usage based estimates of propellant released per month in Brazil. See calculation process below.

- pMDI sale per month = provided by IQVIA
- Total actuations (Vol) = provided by IQVIA
- Assuming 4 puff per day,
  No. of days a pMDI will last = (Row 2/Row 1)/4
- Each pMDI has ~14g of HFO-1234ze, (average amount of propellant/pMDI)
  HFO per pMDI per day in g/day = 14/(Row 4) (g/day)
- Total HFO from all pMDI in a month (in Gg/month) = (Row 5 * Row 1)*DaysInMonth/1e9